inter.noise
HAMBURG 2016

Enhancing microperforated panel absorption by subdividing the backing airspace into channels and resonators

Weiyun Liu[1]; D. W. Herrin[2]
University of Kentucky, USA

ABSTRACT

Microperforated panel absorbers are easily tuned by varying the depth of the airspace behind the panel. In addition, it has been shown that subdividing the airspace behind the panel into a number of smaller cavities improves the microperforated panel absorber performance by preventing grazing wave propagation in the vicinity of the panel. In this work, different strategies for subdividing the airspace and varying the cavity depth behind the microperforated panel are considered. These include multi-depth channels, Helmholtz resonators, tapered or conical channels, and double leaf configurations. In each case, the absorbers are modeled using plane wave strategies, and normal incident sound absorption is measured in an impedance tube. Following this, the absorbers were implemented inside of a small enclosure and the insertion loss for the different treatments are compared. Sound absorbers are developed which greatly improve the broadband frequency attenuation compared to the unpartitioned case.

Keywords: Microperforated Panels, Sound Absorption
I-INCE Classification of Subjects Number(s): 35.3, 35.6

1. INTRODUCTION

Sound absorbing materials like fibers and foams are commonly used to reduce the noise in the mid and high frequency ranges in industrial applications. Though inexpensive and effective, there are drawbacks. Fibers and foams are flammable when they soak up oils and other contaminants and are not suitable for high temperature applications. They may be covered but durable covers adversely affect the performance. When exposed to weather, fibers and foams generally cannot be used due to durability concerns. In schools, health facilities, and food processing plants, fibers are not recommended since particles may dislodge and enter the air passages over time.

For all of these reasons, microperforated panel (MPP) absorbers are increasing in popularity because they are fiber free, rugged, cleanable, and tunable. MPP have perforation sizes on the order of 0.1 to 1 mm. First generation MPP used circular perforations but second generation MPP now use a variety of different perforation schemes.

Due to the small perforation size, sound is attenuated via viscous friction in the holes. Frictional losses are greater when the acoustic particle velocity is high in the holes. Since the acoustic particle velocity is negligible near machine or enclosure surfaces, the MPP is normally spaced at some distance away from a hard surface. Attenuation will be highest when the MPP is placed approximately 1/4, 3/4, 5/4 … wavelength away from a surface to maximize the particle velocity in the perforations. Hence, an MPP sound absorber should be considered as a combination of the MPP plus the backing air cavity.

Due to packaging constraints, the volume of the backing airspace is limited. Over 40 years ago, Wirt[1] proposed several options for dividing a cavity behind a resistive panel absorber. Though not specifically for the MPP, the concepts he recommended are directly transferable to MPP absorbers. Concepts included variable length channels, cones, and Helmholtz resonators.

Several of these concepts have been implemented by MPP researchers. Hua et al.[2] looked at a three-channel and conical backing that was analogous to a Helmholtz resonator. In concurrent work, Park[3] positioned Helmholtz resonators behind a MPP to enhance the lower frequency attenuation.

[1] weiyun.liu@uky.edu
[2] dherrin@engr.uky.edu

Zhao and Fan[4] placed thin plates in the backing airspace having low frequency resonances. The effect is similar to placing a Helmholtz resonator behind the MPP. Zhang and Gu[5], Sakagami et al.[6-7] and Wang et al.[8] considered double leaf configurations.

There is a second reason for integrating channels or resonators into the airspace. Liu and Herrin[9] demonstrated that partitioning the backing airspace greatly improves the sound absorption by preventing grazing wave propagation behind the MPP. They demonstrated that the sound attenuation was increased significantly by partitioning the backing air space for a small enclosure treated on one side. Recall that MPP absorbers are most effective if the particle velocity is high in the perforations. Partitioning forces normal incident propagation behind and, as a result, just in front of the MPP as well.]

This paper will examine a few of the many different backing concepts that may be used to partition a backing airspace and enhance MPP absorber attenuation. Concepts considered include 1) an unpartitioned airspace, 2) a partitioned airspace, 3) a partitioned airspace with Helmholtz resonators, 4) tapered channels with Helmholtz resonators, and 5) a double leaf configuration with partitioning between leaves. The sound absorption for each concept is simulated using plane wave models and compared with impedance tube measurements. Following this, insertion loss results are examined for each of the concepts placed implemented at one end of a small enclosure.

2. DETERMINATION OF TRANSFER IMPEDANCE

The MPP is normally modeled as a transfer or series impedance which is defined as the difference in acoustic pressure on both sides of the MPP divided by the particle velocity. Particle velocity is assumed to be equal on both sides of the panel. This is a reasonable assumption so long as the panel is thin. Hence, transfer impedance can be written as

$$z_{tr} = \frac{p_1 - p_2}{u} \tag{1}$$

where p_1 and p_2 are the respective acoustic pressures, u is the particle velocity, and S is the cross-sectional area of the panel as shown in Figure 1. The transfer impedance is most simply measured using the impedance difference method[10].

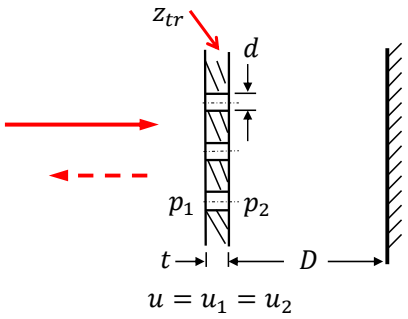

Figure 1 – Schematic of micorperforated panel and backing cavity

Maa[11] first developed MPP absorbers with high temperature and flow environments in mind. In the course of his work, he developed equations to characterize MPP absorbers; first for circular holes and later for elliptical shaped perforations. His developed equations have been the basis for much of the MPP work in the intervening years.

Expressing Maa's equation in the form suggested by researchers at KTH[12] and neglecting flow, the real (r_c) and imaginary (x_c) parts of the transfer impedance (z_{tr}) for circular perforations, can be expressed as

$$r_c = \mathrm{Re}\left(\frac{j\omega t}{\sigma c}\left(1 - \frac{2}{\kappa\sqrt{-j}}\frac{J_1\left(\kappa\sqrt{-j}\right)}{J_0\left(\kappa\sqrt{-j}\right)}\right)^{-1}\right) + \frac{2\beta R_s}{\sigma\rho c} \tag{2}$$

and

$$x_c = \mathrm{Im}\left(\frac{j\omega t}{\sigma c}\left(1 - \frac{2}{\kappa\sqrt{-j}}\frac{J_1\left(\kappa\sqrt{-j}\right)}{J_0\left(\kappa\sqrt{-j}\right)}\right)^{-1}\right) + \frac{0.85d\omega}{\sigma c} \tag{3}$$

for a panel with hole diameter d, porosity σ and thickness t. κ is the dimensionless shear wave number which relates the hole diameter to the viscous boundary layer thickness. It is expressed as

$$\kappa = d\sqrt{\omega/4\nu} \tag{4}$$

ν, ρ and c are the kinematic viscosity, mass density, and speed of sound of the medium respectively. J_0 and J_1 are zeroth and first order Bessel functions of the first kind respectively. R_s is the surface resistance and is defined as

$$R_s = \frac{\sqrt{2}}{2}\sqrt{\eta\rho\omega} \tag{5}$$

where η is the dynamic viscosity. β is equal to 2 for holes with rounded edges and 4 for holes with sharp edges. The above equations are for circular holes though researchers at KTH have developed similar equations for elliptical shaped slits. Li et al.[13] considered the vibration of the MPP. Though neglected in this discussion, those considerations are likely important especially when the MPP is placed in a small enclosure.

The impedance of the perforate plus backing cavity is

$$z = r_c + x_c + \cot(\omega D) \tag{6}$$

where D is the cavity depth. Once the surface impedance (Z) is determined, the normal incident absorption coefficient can be expressed as

$$\alpha = \frac{4Z_R}{(1+Z_R)^2 + Z_I^2} \tag{7}$$

where Z_R and Z_I are the real and imaginary parts of the surface impedance (z) in Equation (6).

3. PLANE WAVE SIMULATION OF MPP AND BACKING AIRSPACE

The backing is most easily modeled using transfer matrix theory[14]. A transfer matrix relates the sound pressure and volume velocity from one to the other side of an acoustic element. Hence,

$$\begin{Bmatrix} p_1 \\ S_1 u_1 \end{Bmatrix} = \begin{bmatrix} T_{11} & T_{12} \\ T_{21} & T_{22} \end{bmatrix} \begin{Bmatrix} p_2 \\ S_2 u_2 \end{Bmatrix} \tag{8}$$

where T_{11}, T_{12}, T_{21}, and T_{22} are the transfer matrix elements. S_1 and S_2 are the cross-sectional area at different points in the channel. The transfer matrix for a MPP is given by

$$[T_{tr}] = \begin{bmatrix} 1 & z_{tr}/S \\ 0 & 1 \end{bmatrix} . \tag{9}$$

where z_{tr} is the transfer impedance. The transfer matrix for a straight duct can be expressed as

$$[T_{sd}] = \begin{bmatrix} \cos(kL) & jz_c/S\sin(kL) \\ jS\sin(kL)/z_c & \cos(kL) \end{bmatrix} \tag{10}$$

where k is the acoustic wavenumber and L is the length of the duct. A cone or tapered duct can be modeled as a series of straight ducts of decreasing or increasing cross-section using Equation (10). Alternatively, a transfer matrix for a cone is available in Munjal's text[14].

The transfer matrix for a side branch can be expressed as

$$[T_{br}] = \begin{bmatrix} 1 & 1 \\ S/z_{br} & 1 \end{bmatrix} \tag{11}$$

where z_{br} is the side branch impedance. The impedance for a side branch can be determined by using the above equations. A transfer matrix is developed from the start to the termination of the side branch. Assuming that the termination of the side branch is rigid, the side branch impedance (z_{br}) can be expressed as

$$z_{br} = \frac{T_{11}}{T_{21}} \tag{12}$$

Each of the designs considered consist of the aforementioned basic elements.

4. MPP BACKING DESIGNS

The different MPP backing designs evaluated consist of those shown in Figure 2. Dimensions are included in Figure 2. Concepts include:

1. Empty airspace.
2. Helmholtz resonator in channel.
3. Tapered partition.
4. Double leaf MPP with panel separation distance of 12 mm.

Concept 1 may be considered the baseline configuration. Concepts 2 and 3 though different in appearance are functionally very similar to one another. In both cases, the lower frequency sound absorption is a result of a Helmholtz resonator in the backing cavity. For Concept 3, the opening at the end of the tapered channel forms a Helmholtz resonator which utilizes the volume on the other side of the tapered channel. Concept 4 consisted of a double leaf MPP. Honeycomb was positioned and epoxied between the two channels. The resulting MPP absorber is much sturdier than the other concepts.

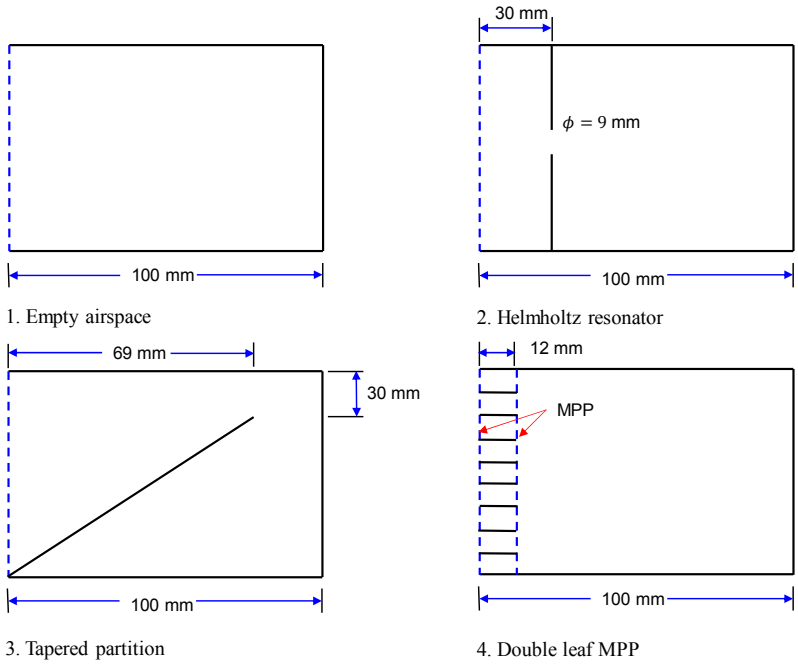

Figure 2 – Schematic of different backing cavity design concepts

The plane wave models for each of the cases are shown in Figure 3. The basic muffler elements are indicated using different colors. Concepts 1 and 4 are straightforward to model. Concept 2 can be modeled either as a combination of 3 straight ducts (as shown) or as a duct connected to a Helmholtz resonator. Concept 3 consists of a linear changing area for the tapered duct shown in blue. The area change can be simulated using a series of straight ducts of linearly decreasing area. At the end of the tapered portion, the impedances of a short duct (shown in yellow) and another tapered duct (shown in green) with linearly decreasing area are in parallel with one another.

Measured and plane wave simulated sound absorption are compared for each of the concepts in Figure 4. The panels used were of the micro-slit type. Maa's theory compares well with measurement when the perforation diameter, porosity, and thickness are selected to be 0.25 mm, 1.8%, and 1 mm respectively. The sound absorption curve shown for Concept 1 is typical for MPP

absorbers. Notice that the MPP absorber is a banded sound absorber and that the sound absorption is lower above 1000 Hz. Concepts 2 (Helmholtz resonator) and 3 (tapered partition) show an improved lower frequency sound absorption due to the Helmholtz resonator. Recall that the Helmholtz frequency is governed by the neck length, neck area, and adjoining cavity volume. Note that the Helmholtz resonance frequency is lower for Concept 2 than Concept 3. This is primarily due to the smaller neck area (shown in green) for Concept 2. In addition, Concept 2 has excellent sound absorption above 1000 Hz due to the shorter cavity depth (shown in blue). However, the sound absorption between 300 and 800 Hz is decreased. Concept 4 (double leaf MPP) shows improved sound absorption at the low frequencies and somewhat better performance in the mid-frequency range compared to Concept 1.

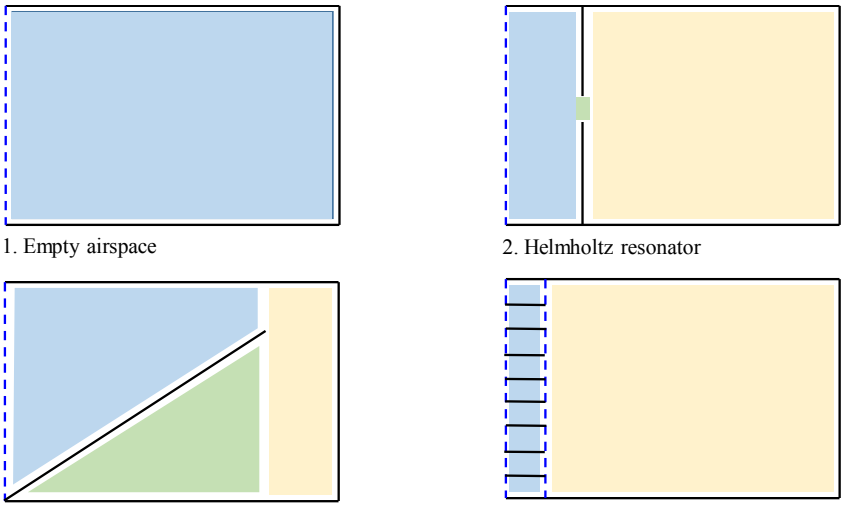

1. Empty airspace

2. Helmholtz resonator

3. Tapered partition

4. Double leaf MPP

Figure 3 – Plane wave models of design concepts

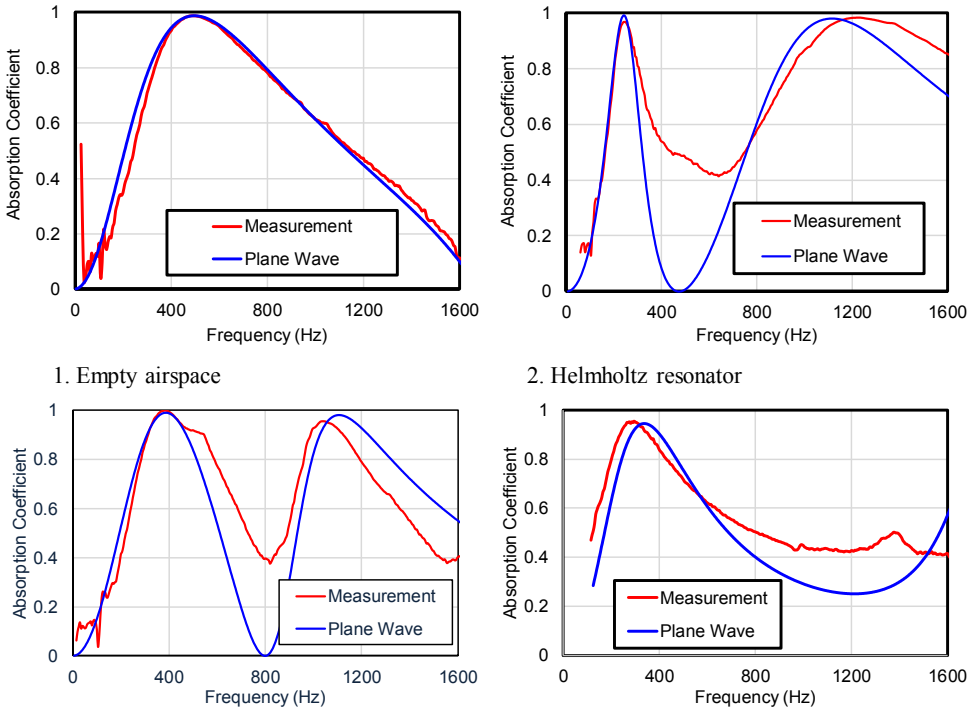

1. Empty airspace

2. Helmholtz resonator

3. Tapered partition

4. Double leaf MPP

Figure 4 – Comparison of measured and plane wave simulated sound absorption for four concepts

5. SMALL ENCLOSURE RESULTS

The different MPP backing concepts were positioned at the end of a small enclosure to assess their performance with three-dimensional wave propagation. A schematic of the enclosure is shown in Figure 5. A loudspeaker was connected to the 970×580×410 mm^3 enclosure on one side via a short tube. Measurements were made on a plane 50 mm from the treatment at 12 positions. For each design concept, the spatially averaged sound pressure was determined on the plane and compared with the spatially averaged sound pressure for the untreated (no MPP present) enclosure. Since the enclosure is highly resonant, the insertion loss was first computed narrowband and then a 200 Hz running average was used to smooth the data for comparison sake.

Five different cases were considered. They are labelled accordingly:

A. No partitioning – The airspace behind the MPP is empty.
B. Partitioned – The airspace behind the MPP is partitioned.
C. Partitioned with alternating Helmholtz resonators – The airspace behind the MPP is partitioned. Helmholtz resonators (Concept 2) and empty channels (Concept 1) are alternated.
D. Partitioned with alternating tapered ducts - The airspace behind the MPP is partitioned. Tapered partitions (Concept 3) and empty channels (Concept 1) are alternated.
E. Double leaf MPP – A double leaf MPP with separation distance of 12 mm between layers is used. Honeycomb partitioning is epoxied between the two MPP layers. The cavity is empty behind the MPP.

For cases B, C, and D, partitions were 99×95 mm^2.

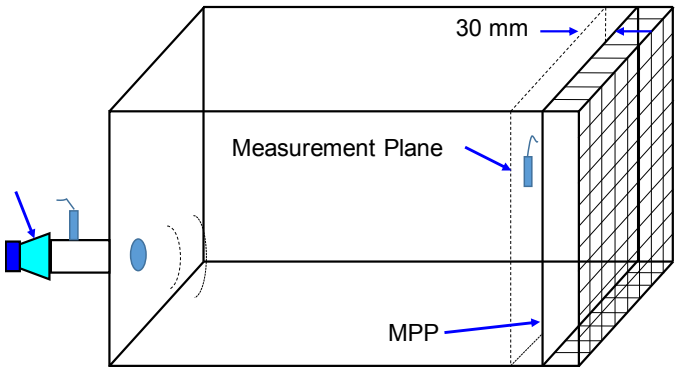

Figure 5 – Schematic showing small enclosure and MPP placement

Figure 6 shows the insertion loss comparisons. By comparing the *No Partitioning* and *Partitioned* cases, it can be observed that partitioning improves the attenuation at frequencies below 500 Hz. This is anticipated since the first cross modes occur at approximately 295 Hz and 420 Hz. Partitioning will especially improve the attenuation at these frequencies since sound waves will be grazing in the unpartitioned case. The *Partitioned with Alternating Helmholtz Resonator* case also improves upon the baseline (*No Partitioning*) at low frequencies. However, the effect due to the Helmholtz resonators at low frequencies is minimal. Also, note that the reduced cavity depth of 30 mm due to the added plate greatly improves the high frequency performance of the sound absorber. The *Partitioned with Alternating Tapered Ducts* case has a performance similar to the *Partitioned with Alternating Helmholtz Resonator* case. However, the attenuation above 1000 Hz is roughly 2 dB lower. The *double leaf MPP* performs similar to the baseline case at low frequencies, but the attenuation is improved between 2 and 5 dB at higher frequencies.

Both the MPP and the partitions themselves likely have lower frequency structural resonances that may improve or degrade the performance. The *double leaf MPP* construction is much sturdier than the other case and so structural resonances are less likely in that case. Also, note that the insertion loss is negative between 450 and 700 Hz. This is likely due to the size of box cavity changing with the added treatments.

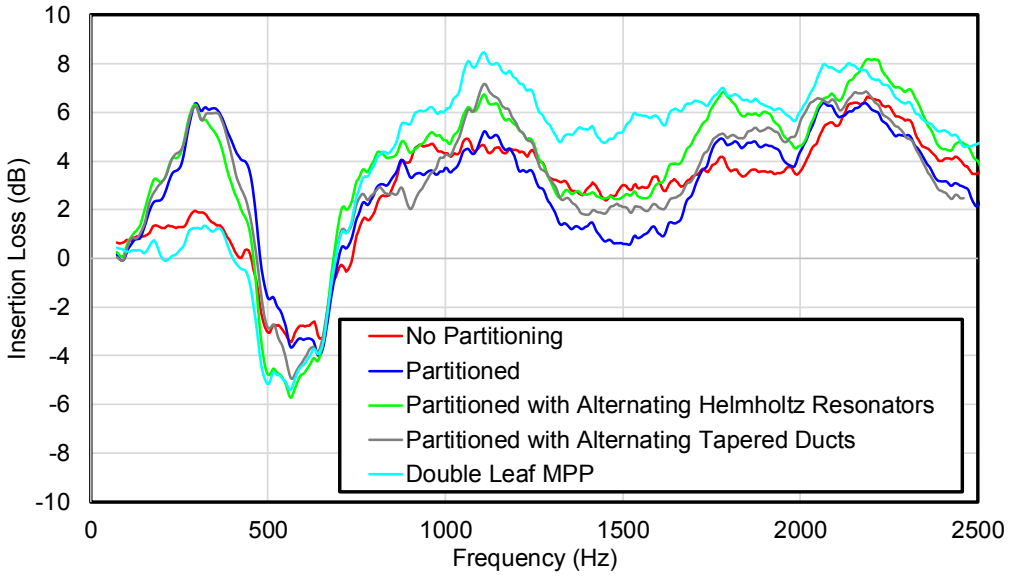

Figure 6 – Schematic showing small enclosure and MPP placement

6. CONCLUSIONS

In this study, the design space for subdividing the air space behind an MPP absorber has been explored. Strategies considered included adding Helmholtz resonators and also tapered ducts. It has been demonstrated that the effect of partitioning appears to be more advantageous than the addition of resonators particularly at the lower frequencies. Shorter cavity depths can pay dividends at higher frequencies. It was also demonstrated that a sturdy double leaf configuration could similarly improve the high frequency performance.

ACKNOWLEDGEMENTS

The authors gratefully acknowledge the support of the Vibro-Acoustics Consortium for this work.

REFERENCES

1. Wirt, L.S., Sound-Absorptive Materials to Meet Special Requirements, Journal of the Acoustical Society of America, 1975; 57(1), pp. 126-143.
2. Hua, X., Herrin, D. W., and Jackson, P., Enhancing the Performance of Microperforated Panel Absorbers by Designing Custom Backings, SAE International Journal of Passenger Cars - Mechanical Systems, 2013; Vol. 6, No. 2.
3. Park, S-H, Acoustic properties of micro-perforated panel absorbers backed by Helmholtz resonators for the improvement of low-frequency sound absorption, Journal of Sound and Vibration 2013, Vol. 332, pp. 4895–4911.
4. Zhao, X. and Fan, X., Enhancing low frequency sound absorption of micro-perforated panel absorbers by using mechanical impedance plates, Applied Acoustics, 2015; Vol. 88, pp. 123-128.
5. Zhang, Z. M. and Gu, X. T., The theoretical and application study on a double layer Microperforated sound absorption structure, Journal of Sound and Vibration, 1998; Vol. 215, No. 3, pp. 399-405.
6. Sakagami, K., Morimoto, M. and Koike, W., A numerical study of double-leaf microperforated panel Absorbers, Applied Acoustics, 2006; Vol. 67, pp. 609-619.
7. Sakagami, K., Yairi, M. and Morimoto, M., Multiple-leaf sound absorbers with microperforated panels: an overview, Acoustics Australia, 2010; Vol. 38, No. 2, pp. 76-81.
8. Wang, W., Wick, R., and Herrin, D. W., Designer backings to improve microperforated panel absorber performance, InterNoise 2015, San Francisco, CA, August 9-12, 2015.
9. Liu, J. and Herrin, D. W., Enhancing micro-perforated panel attenuation by partitioning the adjoining cavity, Applied Acoustics, 2010; Vo. 71, pp. 120-127.
10. Wu, T. W, Cheng, C. Y. R., and Tao, Z., Boundary element analysis of packed silencers with protective cloth and embedded thin surfaces. Journal of Sound and Vibration, 2003; Vol. 261, No. 1, pp. 1–15.

11. Maa, D. Y., Theory and design of microperforated-panel sound-absorbing construction, Scientia Sinica XVIII, 1975; pp. 55-71.
12. Allam, S., Guo, Y., and Åbom, M., Acoustical Study of Micro-Perforated Plates for Vehicle Applications, SAE Noise and Vibration Conference, Paper No. 2009-01-2037, St. Charles, IL, 2009.
13. Li, C., Cazzolato, B. and Zander, A., Acoustic impedance of micro perforated membranes: Velocity continuity condition at the perforation boundary, Journal of the Acoustical Society of America, 2016; Vol. 139, No. 1, pp.93-103.
14. Munjal, M.L., Acoustics of Ducts and Mufflers, 2nd Edition, John Wiley & Sons, Ltd., West Sussex, United Kingdom, 2014.